

Anisotropic growth of indium antimonide nanostructures

J.F. Zhou, Z. Chen, L.B. He, C.H. Xu, L. Yang, M. Han^a, and G.H. Wang

National Laboratory of Solid State Microstructures and Department of Materials Science and Engineering, Nanjing University, Nanjing 210093, P.R. China

Received 24 July 2006 / Received in final form 21 September 2006

Published online 24 May 2007 – © EDP Sciences, Società Italiana di Fisica, Springer-Verlag 2007

Abstract. InSb nanostructures have been synthesized by the use of gas aggregation process. Nanoparticles with different shapes are obtained by controlling the growth and deposition temperature of the InSb nanoclusters. Triangular nanocrystals are commonly observed when the clusters are extracted from the condensation chamber of the source and deposited on the room temperature substrate at high vacuum. When the deposition is performed inside the condensation chamber at high temperature near the melting point of bulk InSb, nanoparticles formed on the substrate surface show several kinds of 3-dimensional morphologies, such as triangular or rectangular prisms, as well as hexagonal tablets. Keeping the same conditions for the cluster source operation and deposition, after long time growth, nanorods with hexagonal and quadrangular cross sections are formed through vapor-liquid-solid (VLS) process. The origin of the difference on the morphologies and shapes of the nanostructures is attributed to the anisotropic growth of InSb, which is temperature dependent.

PACS. 61.46.-w Nanoscale materials – 81.07.-b Nanoscale materials and structures: fabrication and characterization

1 Introduction

Indium antimonide, with a band gap of 0.17 eV at 300 K, has been extensively used for infrared astronomy and thermal imaging [1]. Moreover, InSb has the highest electron mobility among all semiconductor materials, which shows potential applications in fabrication of high-speed transistors [2,3,7]. Meanwhile, blue shift of photoluminescence (PL) has been discovered from InSb quantum dots [4,5] and elucidated to the three dimensional confinement. Many researches have been carried out on how to get InSb quantum dots [4–8] with controlled size and morphology so as to get infrared light emitter with tunable wavelength. However, up to now few have been reported on the synthesis of one-dimensional nanostructures of InSb, despite the many successes on other semiconductor one-dimensional materials, such as ZnO, Si and Ge. Recently, InSb nanowires were discovered on the ion beam-sputtered InSb (001) surface [10]. Long InSb nanowires were also synthesized with asbestos matrix template [9]. However, there were no reports that the vapor-liquid-solid (VLS) method was used for InSb one-dimensional nanostructure formation. VLS process is now a common method for semiconductor nanowire synthesis. According to this mechanism, the anisotropic crystal growth is promoted by the presence of the liquid alloy/solid interface. The process supplies the reactants in a vapor phase. They react with a liquid metallic seed particle placed on a substrate and form

a liquid alloy droplet, which always occurs on the tip of the grown wire. One-dimensional nanostructure is gradually formed with the component separation from the saturated droplet on the tip. In this paper, we report on the fabrication of InSb nanoparticles in different morphologies and shapes, as well as one-dimensional InSb nanorods. The formation of InSb nanorods is considered as an anisotropic crystal growth via VLS process. Metal droplet of In, which comes from the high temperature decomposition of InSb, acts as the catalytic seed.

2 Experimentals

The syntheses are performed in a gas aggregation cluster source. Details of the experimental equipment can be referred to reference [11]. Stoichiometric InSb powder is evaporated in a BN oven to generate gaseous InSb. Inert gas (helium or argon) is introduced as carrier gas to stimulate the nucleation of InSb clusters and extract the products from the nucleation zone. The evaporation temperature varies around the melting point of InSb powder (520 °C). Amorphous carbon films supported with copper grids are used as substrates for transmission electron microscopy (TEM) characterization. Si wafers are also used as substrates, which are mounted inside the effusion hole of the evaporation oven so as to collect specimens directly grown on it under high temperature. The specimens are then used for scanning electron microscopy (SEM) observation.

^a e-mail: sjhanmin@nju.edu.cn

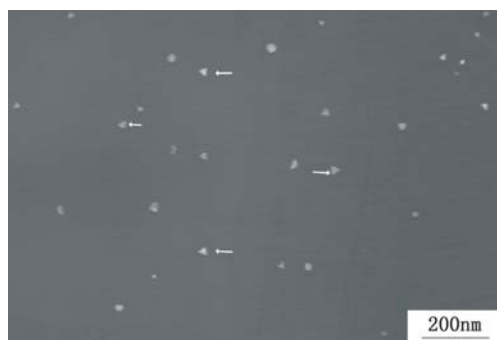


Fig. 1. TEM image of InSb nanoparticles deposited on an amorphous carbon film at room temperature.

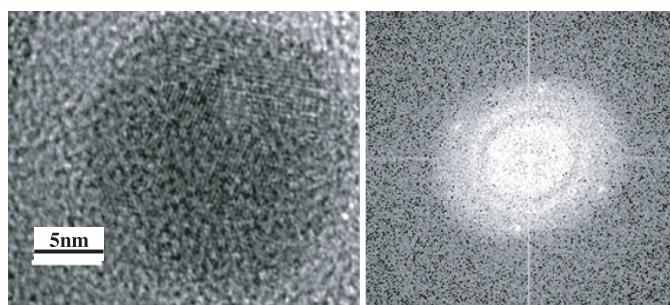


Fig. 2. HRTEM image and the corresponding (FFT) 2D power spectrum of a spherical nanoparticle.

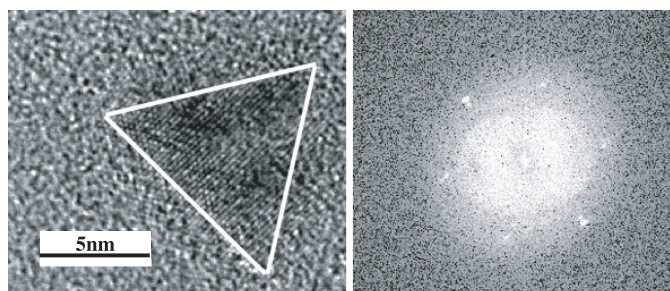


Fig. 3. HRTEM image and the corresponding (FFT) 2D power spectrum of a triangular nanoparticle.

3 Result and discussion

When the evaporation temperature is kept at 650 °C and the He gas pressure in the aggregation chamber is kept at 1 Torr, an InSb nanocluster-based specimen is deposited. The clusters are extracted from the aggregation chamber and deposited on the amorphous carbon films in a high vacuum chamber that is separated from the aggregation chamber by a skimmer. The deposition is performed for 5 seconds at room temperature and the specimen is characterized with TEM. Two kinds of nanoparticles, with either spherical shapes or triangular shapes (indicated by the arrows) can be distinguished from the specimen, as shown in Figure 1. The particle size is between 10 nm and 20 nm. Both kinds of nanoparticles are analyzed by high resolution TEM (HRTEM) (Figs. 2 and 3) to characterize their internal structures. As it can be seen, distinct lattices can be identified in both of the HRTEM images

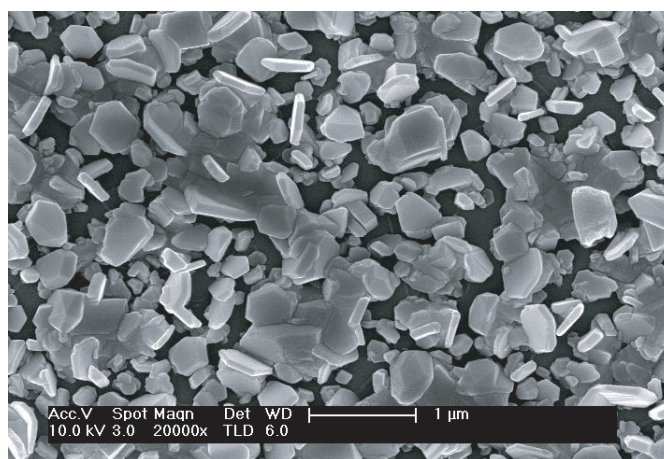


Fig. 4. SEM image shows InSb hexagonal tablets distributed randomly among irregular particles.

of the nanoparticles. However, the 2D power spectra from the fast Fourier transform (FFT) of the HRTEM images illustrate different symmetries: the spherical particle has four-fold symmetry and the triangular particle owns three-fold symmetry.

Usually, excess In atoms are precipitated in InSb film during the fabrication process [12]. In bulk, Indium crystal belongs to tetragonal system with no three-fold symmetry, while InSb has a zinc blend structure and owns three-fold symmetry along (111) direction. Judged from the symmetries obtained from the 2D power spectra of the HRTEM images, the triangular particles are InSb nanocrystals and the spherical particles are In nanocrystals aggregated from the precipitation of excess In atoms. In fact, crystalline In and crystalline InSb can coexist in one big particle [8]. In crystal growth, crystal plane with the lowest surface energy has the highest growth speed. For InSb with a face-centered cubic structure, (111) is such a crystal plane. When this plane is exposed, the crystal often takes a triangular appearance.

If we decrease the evaporation temperature to 520 °C and keep the carrier gas pressure at 5 Pa, hexagonal tablets can be discovered with scanning electron microscopy (SEM) from the specimen deposited for 30 minutes on the silicon wafer near the evaporation oven, as shown in Figure 4. The hexagonal tablets are randomly distributed among other irregular shaped particles; they can be either parallel or perpendicular to the substrate surface. Their sizes reach hundreds of nanometer. The hexagonal structure can be ascribed to the evolution of triangular nanoparticle. Since the specimen was collected in the condensation zone before being extracted to differentially pumped high vacuum zone, the deposits may contain a large fraction of very small clusters or even monomers. The growth of the hexagonal crystals can proceed with adsorbing monomers or merging small clusters through Ostwald ripening. As mentioned above, the rapid growth of the (111) plane results in the triangular morphology of the InSb crystal. However, if the rapid growth of the (111) plane is accompanied by the slower growth of the planes

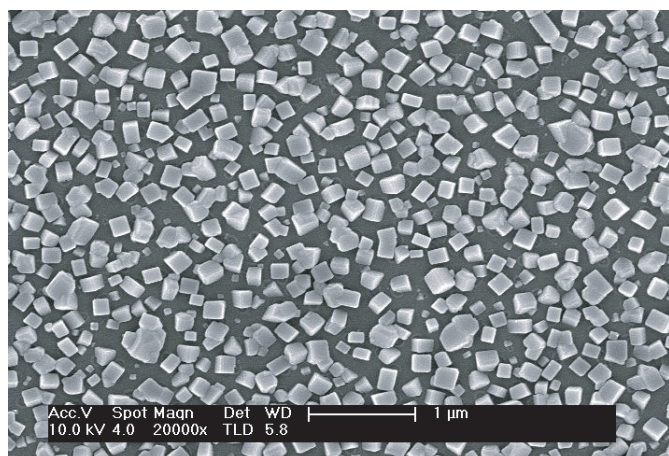


Fig. 5. SEM image showing rectangular-shaped InSb particles.

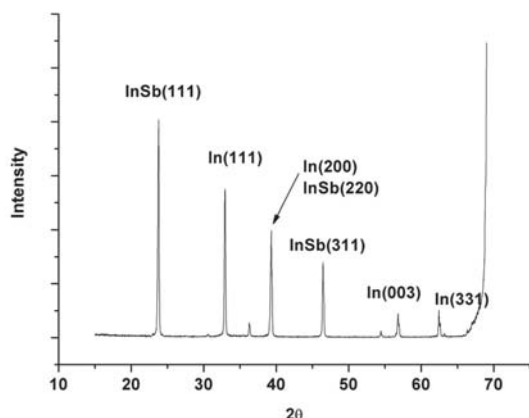


Fig. 6. XRD pattern of film composed of rectangular-shaped InSb particles.

(10 $\bar{1}$), ($\bar{1}$ 01), (1 $\bar{1}$ 0), ($\bar{1}$ 10), (01 $\bar{1}$), (0 $\bar{1}$ 1) that are vertical to this plane, the (111) plane will have a hexagonal shape, because its growth is confined by the development of the {110} planes, which simultaneously grow and enclose a hexagonal area. As a result, hexagonal tablets with (111) top surfaces are formed. On the other hand, if the growth occurs by smaller cluster contact and coalescence, irregular particles will be formed.

Furthermore, if the carrier gas pressure is increased to the order of 200 Pa, rectangular, as well as triangular particles are formed on the Si substrate instead (Fig. 5). Their sizes reach 100 nm with 30 minutes growth. The X-ray diffraction (XRD) pattern of this InSb film exhibits several reflection peaks in the diffraction angle range of 10–70°, which correspond to InSb (111), (311) and In (111), (003), (331) reflections, as shown in Figure 6. For each interplanar spacing, the intensity ratio of the diffraction peak has a typical value of the standard XRD spectrum of InSb or In, except the one that is indicated by an arrow in Figure 6. This reflection corresponds to a 0.229 nm interplanar spacing and has a FWHM (full width at half maximum) of 0.24, which is much broader than others. The broadening of the diffraction peak and the deviation of the intensity ratio may come from the overlap of the InSb

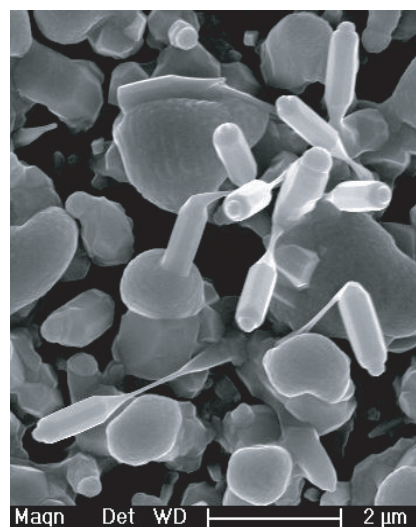


Fig. 7. SEM images showing different shaped InSb nanorods grown from VLS mechanism.

(220) and In (200) reflections, since they locate almost at the same diffraction angle. Therefore, the XRD pattern proves the coexistence of tetragonal In nanocrystals, clustering from the excess In decomposed from InSb, and triangular InSb nanocrystals with zinc blend structure.

Rectangular InSb particles have been observed from nucleation in benzene [7]: they were grown through a free nucleation process and the rectangular shape of the particles comes from the anisotropic growth of InSb crystal. But here it is more evident that the rectangular appearance of the particles should come from the excess indium, considering the XRD pattern of In crystals we observed. The indium growth along (100) direction results in the rectangular shape.

One-dimensional short nanorods are synthesized from a long time growth under high temperature in the aggregation chamber. Figure 7 shows the SEM images of such InSb nanorods. They are formed through a 2 hours' growth. The evaporation temperature is kept at 570 °C, a little higher than that for the formation of rectangular-shaped particles and hexagonal tablets shown in Figures 4 and 5. Ar is used instead of He as carrier gas. The gas pressure in the aggregation chamber is also 200 Pa. From Figure 7, hexagonal prisms can be identified. They have the same symmetries as the InSb nanocrystals mentioned above and may also have the same origin. Large spherical particles are always observed on the top of the nanorod, which may give the evidence of a VLS mechanism growth that controls the nanorod formation. But if such mechanism is really present in the InSb nanorod growth, a deviation from the ordinary VLS process should be considered. In a common VLS process, the droplet on the top of the nanorod is mainly composed of metal catalyst and never contributes to the chemical component of the final solid phase. Here the droplet forms from the excess In. Since the temperature of our experiments is much higher than the melting point of In (156 °C), the droplet is always in liquid phase. In droplet can provide the liquid phase and absorb

Sb from the gas ambient to synthesize InSb component. When InSb is saturated in In droplet it precipitates into solid nanorod under the droplet. Obviously In not only catalyzes the nanorod formation by VLS growth, but also contributes to the chemical component of the final solid.

Finally we discuss briefly about the effect of the substrate temperature. Although the substrate temperature has not been precisely measured, it should certainly be well below the temperature of the evaporation oven. And since the evaporation temperature in our experiment is not so much higher than the melting point of InSb, it is appropriate to assume that the substrate temperature is below the melting point of InSb and changes monotonically with the evaporation temperature. Obviously, to grow InSb nanorod in solid form a substrate temperature well below the melting point of InSb is required. And from our experiments it seems that lower temperature is preferred for an anisotropic growth. However, the temperature should still be high enough to keep the In-rich droplet on top of the nanorod in liquid phase.

In conclusion, under an appropriate temperature below the melting point of InSb, anisotropic growths of InSb induce two kinds of nanostructures with triangular and hexagonal symmetries on morphologies respectively, which have the correspondence with the internal lattice symmetries of In and InSb crystals.

This work is financially supported by the National Nature Science Foundation of China (Grant Nos. 90206033, 60478012, 10274031 and 10021001) and from the Hitech Research and Development Program of China under contact number 2006AA03Z316. Supports from the Analysis and Measurement Foundation of Nanjing University should also be acknowledged.

References

1. T.S. Rao, J.B. Webb, D.C. Houghton, J.M. Baribeau, W.T. Moore, J.P. Noad, *Appl. Phys. Lett.* **53**, 51 (1988)
2. J.-L. Chyi, S. Kalem, N.S. Kumar, C.W. Litton, H. Morkoc, *Appl. Phys. Lett.* **53**, 1092 (1988)
3. J.-L. Chyi, D. Biswas, S.V. Iyer, N.S. Kumar, H. Morkoc, H.Y. Lee, H. Chen, *Appl. Phys. Lett.* **54**, 1016 (1989)
4. Y. Qiu, D. Uhl, *Appl. Phys. Lett.* **84**, 1510 (2004)
5. E. Alphandery, R.J. Nicholas, N.J. Mason, B. Zhang, P. Moeck, G.R. Booker, *Appl. Phys. Lett.* **74**, 2041 (1999)
6. T. Ulzmeier, P.A. Postiga, J. Tamayo, R. Garcia, F. Briones, *Appl. Phys. Lett.* **69**, 2674 (1996)
7. Y.D. Li, Z.Y. Wang, X.F. Duan, G.H. Zhang, C. Wang, *Adv. Mat.* **13**, 145 (2001)
8. D. Besson, M. Treilleux, A. Hoareau, C. Esnouf, *Mat. Sci. Eng. B* **90**, 123 (2002)
9. S.V. Zaitsev-Zotov, Y.A. Kumzerov, Y.A. Firsov, P. Monceau, *J. Phys.: Condens. Matter* **12**, L303 (2000)
10. F. Krok, J.J. Kolodziej, B. Such, P. Piatkowski, M. Szymonski, *Nucl. Instr. Meth. Phys. Res. B* **212**, 264 (2003)
11. J.F. Zhou, Z.L. Li, Y.F. Chen, G.H. Wang, M. Han, *Sol. Stat. Comm.* **133**, 271 (2005)
12. K.G. Guenther, H. Freller, *Z. Naturforsch. A* **16**, 279 (1961)
13. R. Noetzel, J. Temmyo, T. Tamamura, *Nature* **369**, 131 (1994)
14. R. Noetzel, J. Temmyo, H. kamada, T. Furuta, *Appl. Phys. Lett.* **65**, 457 (1994)